Electronic Supporting Information

Sulfate-modified Ti^{IV}–Zr^{IV}-heterometallic germanotungstate used for catalyzing Knoevenagel condensation reaction

Peijun Gong,[a,c] Hailou Li,[a] Junwei Zhao *[b] and Guo-Yu Yang *[a]

[a]*MOE Key Laboratory of Cluster Science, School of Chemistry and Chemical Engineering, Beijing Institute of Technology, Beijing 102488, China*

[b]*Henan Key Laboratory of Polyoxometalate Chemistry, College of Chemistry and Molucular Sciences, Henan University, Kaifeng, Henan 475004, China*

[c]*College of Chemistry and Pharmaceutical Engineering, Huanghuai University, Zhumadian 463000, China*

E-mail: zhaojunwei@henu.edu.cn, ygy@bit.edu.cn

Fig. S10 Comparison of PXRD patterns of **1** before and after the condensation reaction between benzaldehyde and malononitrile.

Table S1 The crystallographic data and structure refinement for **1**.

Table S2 Bond valence sum parameters for W1, Ge1, Zr1, Ti1, S1, O11, O12, O13 and O15 atoms in **1**.

Table S3 Effect of different starting materials on the condensation reaction of benzaldehyde with malononitrile.

Table S4 Comparison of some catalysts for the condensation reaction of benzaldehyde with malononitrile.

Materials and methods

The precursor K_8Na_2[A-α-GeW_9O_{34}]·$25H_2O$ was obtained as previously described and further identified by IR spectroscopy.[1] All other chemicals were commercially purchased and used directly without any purification. IR spectra were collected from the solid sample palletized with KBr on a Bruker VERTEX 70 IR spectrometer in the range 400–4000 cm^{-1}. Powder X-ray diffraction patterns were recorded by Bruker D8 Advance X-ray diffractometer equipped with Cu-Kα radiation (λ = 1.54056 Å). Thermogravimetric (TG) curve was obtained by using Mettler Toledo TG/DSC 1100 analyzer with the heating rate of 10 °C/min in the temperature range of 25−800 °C in the air atmosphere. The GC spectra were obtained on a SHIMADZU GC-2014C.

X-ray Crystallography

A good quality crystal of **1** was selected for data collection on a Bruker APEX II diffractometer equipped with graphite monochromated Mo Kα (λ = 0.71073 Å) at 293(2) K. The structure was solved by the direct method and refined on F^2 by full-matrix least-squares methods using the SHELX 97 program package.[2–3] Lorentz polarization and SADABS corrections were applied. All the hydrogen atoms connected to carbon and nitrogen atoms were generated geometrically and refined isotropically with a riding mode by the default SHELXTL parameters. No hydrogen atoms attached to water molecules were located from the difference Fourier map. However, there are still solvent accessible voids in the check cif reports of crystal structures, indicating that some lattice water molecules or counter cations should exist in their structures that can't be found from the weak residual electron peaks. According to the results of the elemental analysis and TG analysis, thirty-five lattice water molecules and eight $[H_2N(CH_3)_2]^+$ cations are directly added to the molecular formula. Crystallographic data and structure refinements for **1** are listed in Table S1. Crystallographic data and structure refinements for **1** reported in this paper have been deposited in the Cambridge Crystallographic Data Center with CCDC 2385378. These data can be obtained free of charge from the Cambridge Crystallographic Data Centre via www.ccdc. cam.ac.uk/data_request/cif.

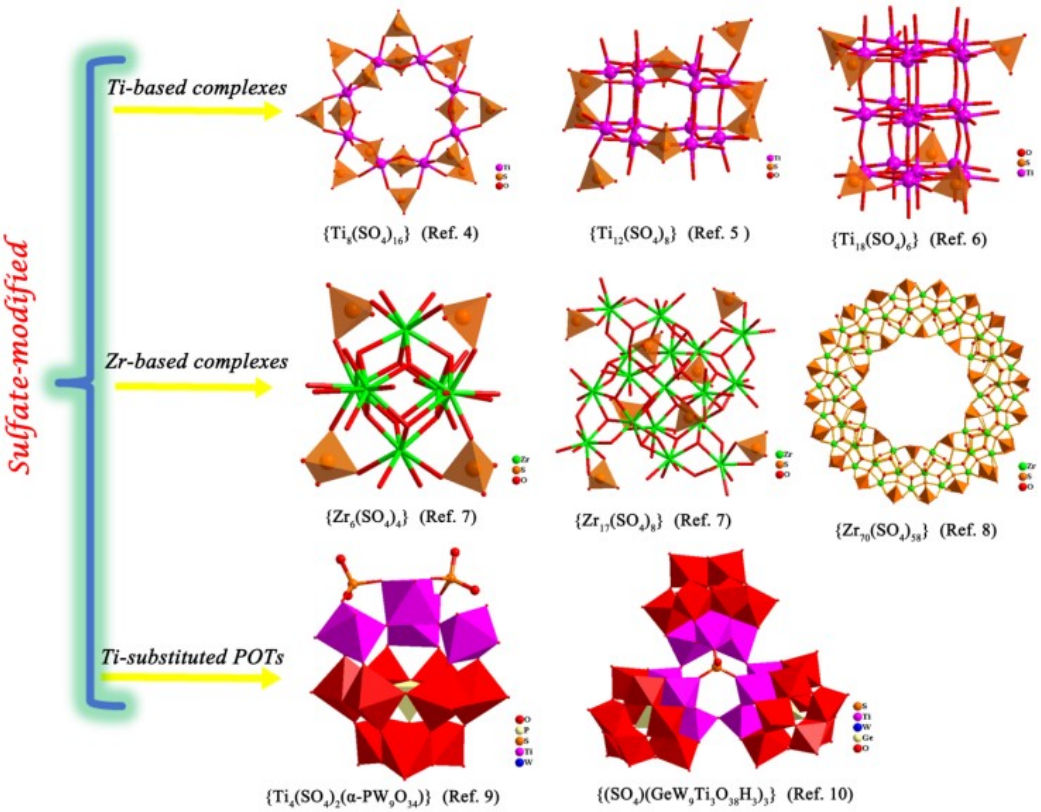

Fig. S1 Summary of some representative sulfate-modified Ti-based complexes, Zr-based complexes and Ti-substituted POTs.

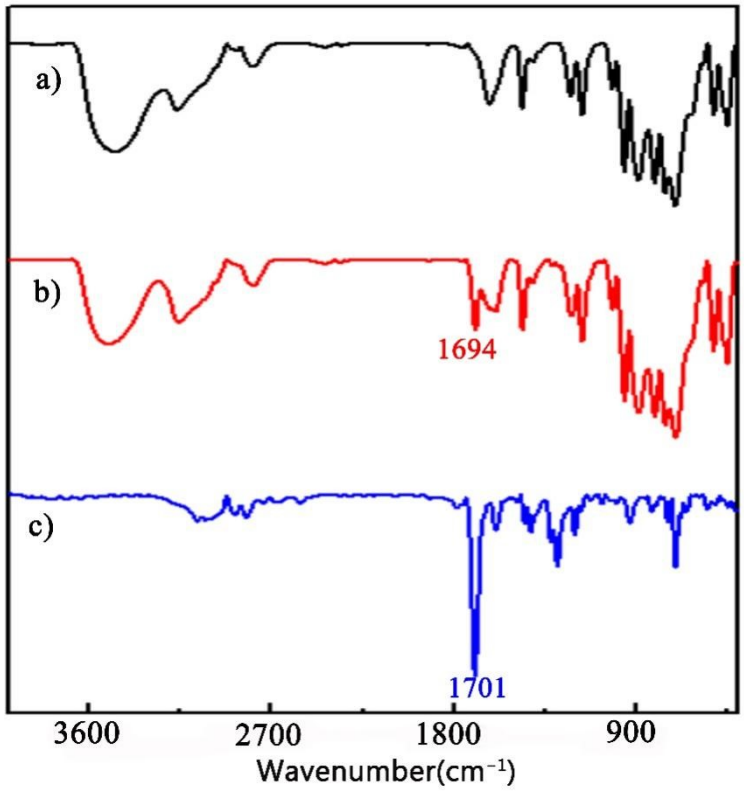

Fig. S2 IR spectra of **1** (a), **1** after impregnation in the substrate benzaldehyde (b) and benzaldehyde (c).

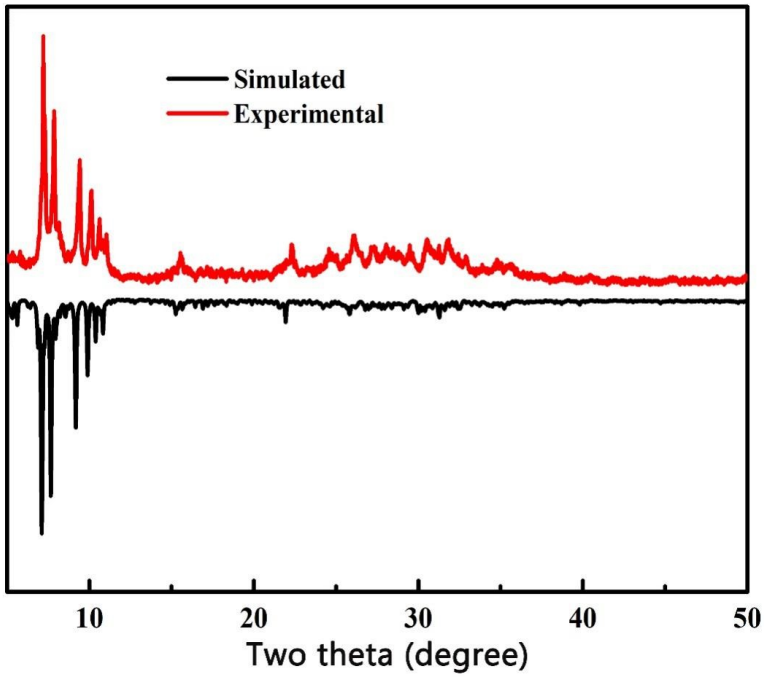

Fig. S3 The experimental and simulated X-ray diffraction patterns of **1**.

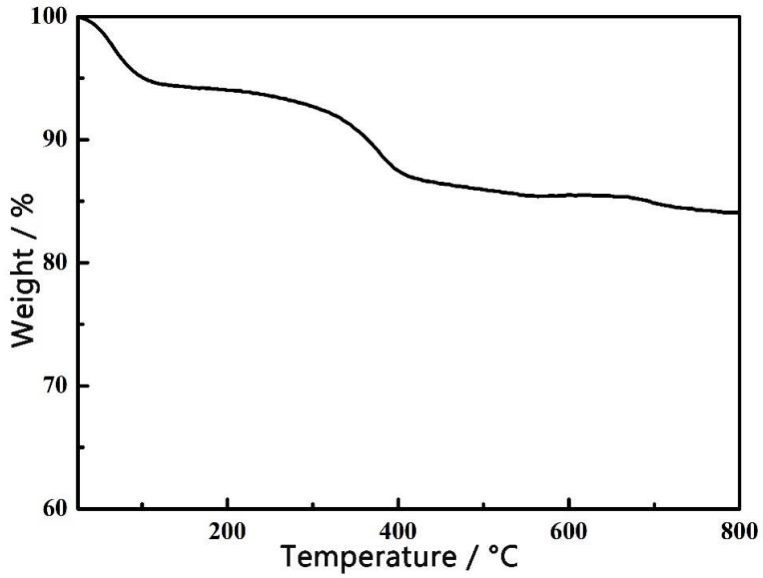

Fig. S4 The TG curve of **1**.

TG Analysis. The TG curve of **1** was obtained by using Mettler Toledo TG/DSC 1100 analyzer with the heating rate of 10 °C/min in the temperature range of 25−800 °C in the air atmosphere. As shown in Fig. S4, the TG curve of **1** shows a two-step weight loss process. The first step weight loss of 7.30 % (calcd. 7.13 %) takes place between 25 and 300 °C, which is attributed to the loss of 47 lattice water molecules and one acetic molecule. The second step weight loss of 8.62% (calcd. 8.15%) occurs in the temperature range of 300–800 °C, which is assigned to the loss of 18.5 dimethylamine groups and the dehydration of 18.5 protons and 4 hydroxyl groups.

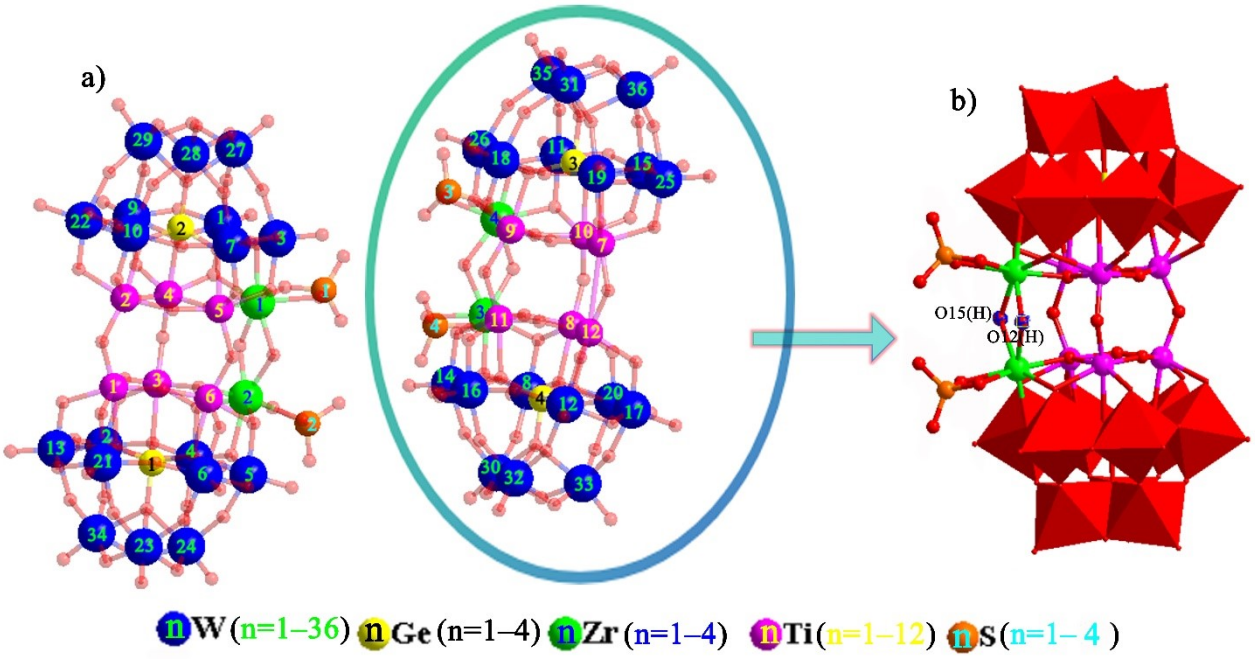

Fig. S5 (a) The molecular structure of **1** with selected atom numbering scheme; (b) One of the two dimeric $[Ti_6Zr_2O_9(OH)_2(SO_4)_2(A\text{-}\alpha\text{-}GeW_9O_{34})_2]^{12-}$ subunits.

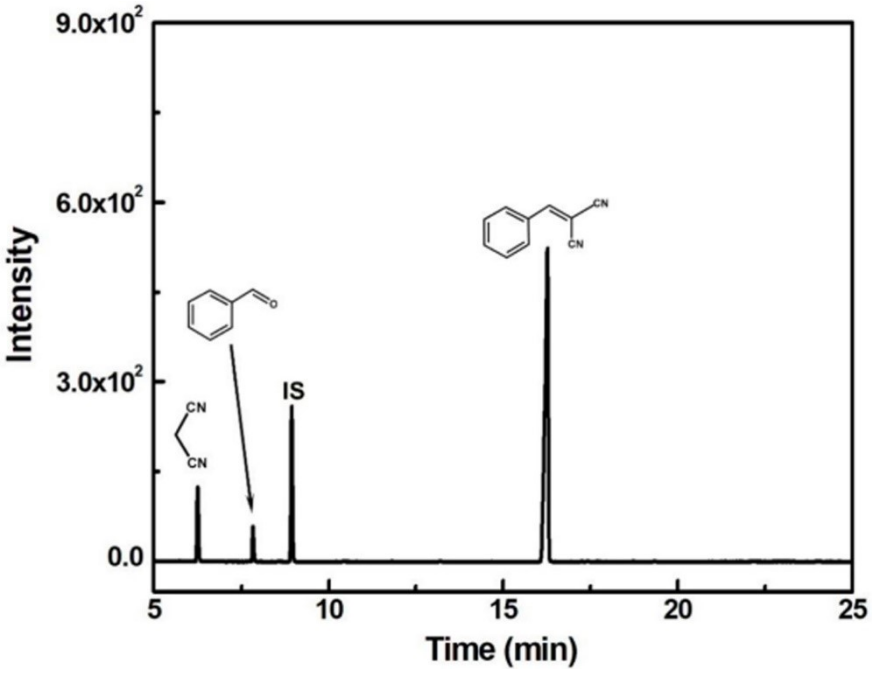

Fig. S6 The Knoevenagel condensation reaction of benzaldehyde and malononitrile detected by GC. Reaction conditions: 0.5 mmol benzaldehyde, 1.0 μmol catalyst, 0.75 mmol malononitrile, 3 mL CH_3OH and 30 °C.

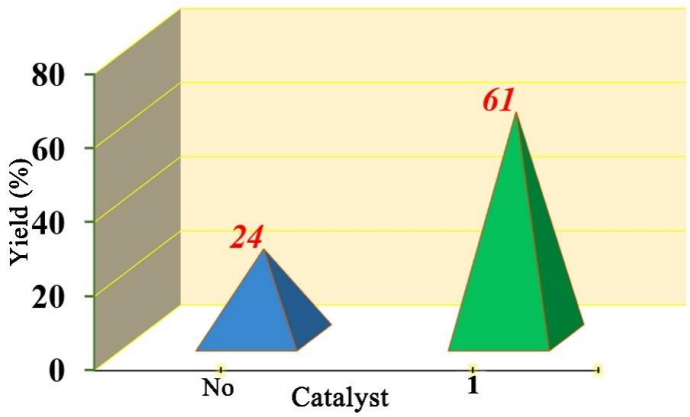

Fig. S7 The comparative experiments under the reaction conditions: 0.5 mmol benzaldehyde, 1.0 μmol catalyst, 0.75 mmol malononitrile and 3 mL CH_3OH, at 30 °C for 30 min.

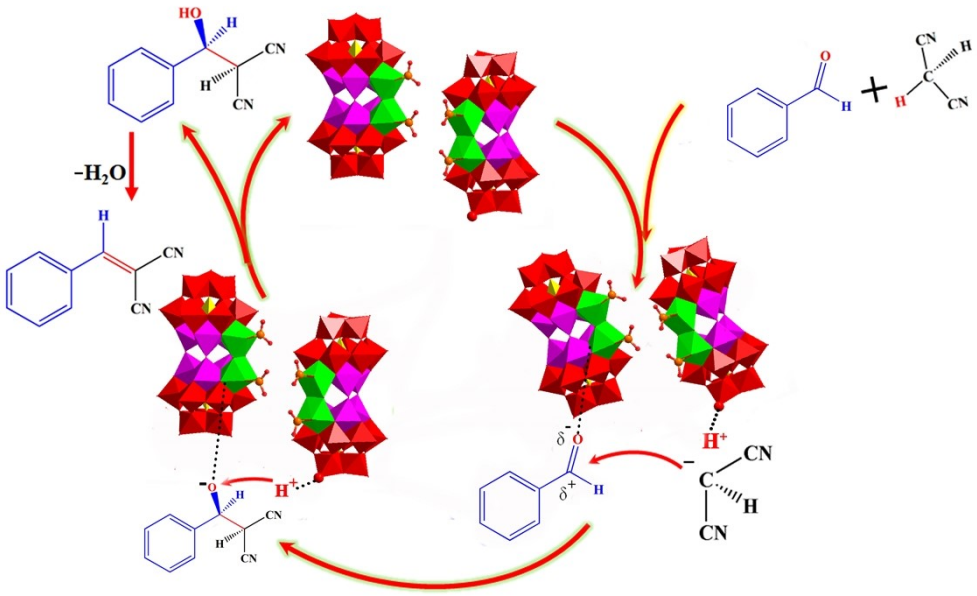

Figure S8. Proposed mechanism for the reaction between benzaldehyde with malononitrile catalyzed by **1**.

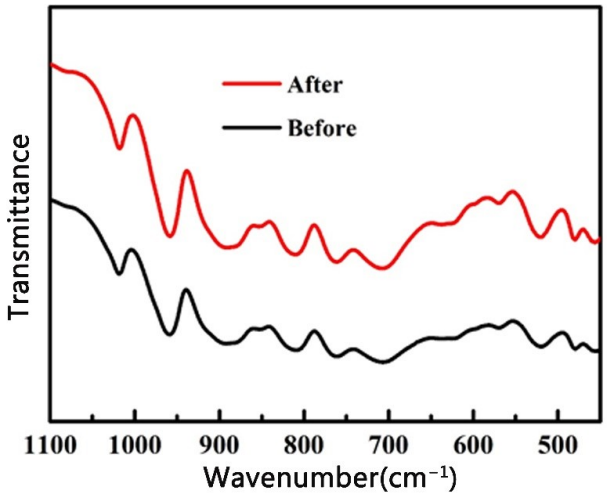

Fig. S9 IR spectra of **1** before and after the Knoevenagel condensation reaction of benzaldehyde with malononitrile**.**

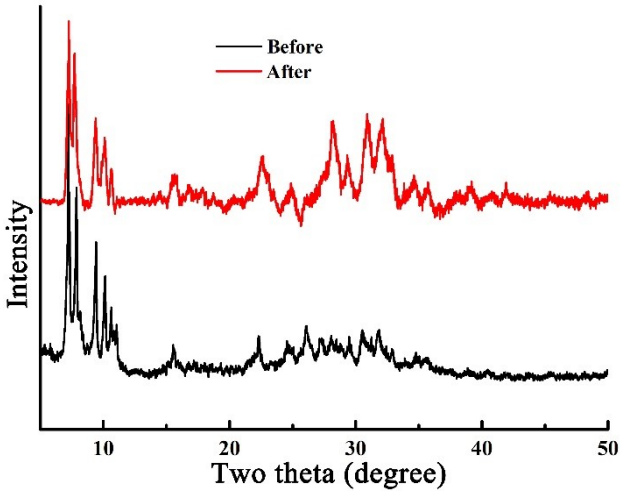

Fig. S10 Comparison of PXRD patterns of **1** before and after the condensation reaction between benzaldehyde and malononitrile.

Table S1. Crystallographic data and structure refinements for **1**.

	1
Empirical formula	$C_{39}H_{250}Ge_4K_{4.5}N_{18.5}NaO_{223}S_4Ti_{12}W_{36}Zr_4$
Formula weight	12723.40
Temperature / K	293(2)
Crystal system	Triclinic
Space group	*P*-1
a [Å]	20.8839(14)
b [Å]	24.4799(15)
c [Å]	25.2479(18)
α [°]	88.621(2)
β [°]	79.799(2)
γ [°]	70.358(2)
V [Å^3]	11955.6(14)
Z	2
ρ_{calcd} [g cm^{-3}]	3.534
μ [mm^{-1}]	18.510
F (000)	11548
Index ranges	$-24 \le h \le 24$, $-29 \le k \le 29$, $-30 \le l \le 30$
Reflections collected/unique	387581 / 42035
R_{int}	0.0585
data/restraints/parameters	42035 / 8 / 2436
Goodness-of-fit on F^2	1.038
R_1, wR_2 [$I > 2\sigma(I)$]	$R_1 = 0.0305$, $wR_2 = 0.0868$
R_1, wR_2 [all data]	$R_1 = 0.0363$, $wR_2 = 0.0897$

Table S2. Bond valence sum parameters for W1, Ge1, Zr1, Ti1, S1, O11, O12, O13 and O15 atoms in **1**.

Bond	Bond lengths (Å)	Bond valence	Bond valence sum
W(1)-O(59)	1.710(6)	1.750	∑(W1) = 6.026
W(1)-O(157)	1.880(6)	1.105	
W(1)-O(57)	1.880(6)	1.105	
W(1)-O(55)	1.922(5)	0.986	
W(1)-O(113)	2.021(6)	0.755	
W(1)-O(111)	2.333(5)	0.325	
Ge(1)-O(137)	1.735(6)	1.036	∑(Ge1) = 4.107
Ge(1)-O(103)	1.737(6)	1.030	
Ge(1)-O(140)	1.739(5)	1.025	
Ge(1)-O(119)	1.742(6)	1.016	
Zr(1)-O(29)	2.096(6)	0.635	∑(Zr1) = 3.792
Zr(1)-O(13)	2.155(6)	0.541	
Zr(1)-O(11)	2.168(6)	0.523	
Zr(1)-O(113)	2.182(6)	0.503	
Zr(1)-O(66)	2.259(6)	0.409	
Zr(1)-O(55)	2.261(6)	0.406	
Zr(1)-O(21)	2.270(6)	0.397	
Zr(1)-O(17)	2.289(6)	0.378	
Ti(1)-O(93)	1.814(6)	1.002	∑(Ti1) = 4.189
Ti(1)-O(22)	1.853(7)	0.902	
Ti(1)-O(28)	1.864(6)	0.876	
Ti(1)-O(82)	2.043(6)	0.540	
Ti(1)-O(62)	2.051(6)	0.528	
Ti(1)-O(140)	2.212(6)	0.341	
S(1)-O(20)	1.448(7)	1.609	∑(S1) = 5.927
S(1)-O(60)	1.451(7)	1.596	
S(1)-O(21)	1.504(6)	1.383	
S(1)-O(17)	1.516(7)	1.339	
O(11)-Zr(1)	2.168(6)	0.552	∑(O11) = 1.075
O(11)-Zr(2)	2.148(6)	0.523	
O(12)-Zr(3)	2.154(6)	0.543	∑(O12) = 1.059
O(12)-Zr(4)	2.173(6)	0.516	
O(13)-Zr(1)	2.155(6)	0.541	∑(O13) = 1.090
O(13)-Zr(2)	2.150(6)	0.549	
O(15)-Zr(3)	2.149(6)	0.550	∑(O15) = 1.087
O(15)-Zr(4)	2.158(6)	0.537	

Table S3. Effect of different starting materials on the condensation reaction of benzaldehyde with malononitrile.

Catalyst	Time (min)	Temp. (°C)	Conv.[a] (%)	Yield[b] (%)

$TiOSO_4$ (Ti^{4+})	120	30	89	10
$ZrOCl_2·8H_2O$ (Zr^{4+})	120	30	90	9
[A-α-$GeW_9O_{34}]^{10-}$+Ti^{4+}+Zr^{4+}	120	30	90	55
1	120	30	94	94

[a] based on benzaldehyde; [b] benzylidenemalononitrile

Table S4. Comparison of some catalysts for the condensation reaction of benzaldehyde with malononitrile.

Compounds	Dosage (μmol)	Time (min)	Temp. (°C)	Yield (%)	Ref.
$\{[(CH_3)_2NH_2]_2[CaZn(TDP)(H_2O)]·3DMF·3H_2O\}n$	30	60	50	78	11
$\{[In_2(BDCP)](Br)\}_n$	75	240	65	99	12
$(NO_3)_{12}$@$[Ln_{132}Ni_{78}(OH)_{292}(IDA)_{48}(CH_3COO)_{96}(NO_3)_{12}(H_2O)_{78}]·Cl_{44}·xH_2O·yCH_3OH$	0.5	180	60	99	13
$H_{27}K_2Na_6(H_2O)_{17}[K(H_2O)(Nb_6O_{19})_2(Nb_6O_{20})(RA)_2]·13H_2O$	8.4	120	60	99	14
$[Co(bix)(H_2O)]\{V_2O_6\}$	10	45	60	> 99	15
$[γ\text{-}SiW_{10}O_{34}(H_2O)_2]_4]^{4-}$	5	150	32	90	16
$Na_8H[A\text{-}PW_9O_{34}]·7H_2O$	2.5	360	25	92	17
$Na_8H[B\text{-}PW_9O_{34}]·19H_2O$	2.5	360	25	89	17
$[H_2N(CH_3)_2]_8Na_8Cs_4H_9[Eu_2SeW_4O_{11}(OH)(H_2O)_4(SbW_9O_{33})(SeW_9O_{33})(Se_{1/2}Sb_{1/2}W_9O_{33})]_2·32H_2O$	0.5	90	30	98	18
$Cs_3Na_5H_{10}[BO(OH)_2Co_9O(OH)(H_2O)_3SiW_6O_{26}(B\text{-}α\text{-}SiW_9O_{34})_2]·11H_2O$	1	60	30	93	19
1	1	120	30	94	This work

References

1. N. Haraguchi, Y. Okaue, T. Isobe and Y. Matsuda, *Inorg. Chem*., 1994, **33**, 1015−1020.

2. G. M. Sheldrick, SHELXL-97, Program for Crystal Structure Refinement, University of Göttingen: Göttingen, Germany, 1997.
3. G. M. Sheldrick, SHELXS-97, Program for Crystal Structure Solution, University of Göttingen: Göttingen, Germany, 1997.
4. Y. L. Fu, Z. W. Xu and F. F. Zhang, *J. Mol. Struct*., 2008, **873**, 168−172.
5. G. Y. Zhang, W. Y. Li, C. Y. Liu, J. Jia, C.-H. Tung and Y. F. Wang, *J. Am. Chem. Soc*., 2017, **140**, 66−69.
6. G. Y. Zhang, C. Y. Liu, D. L. Long, L. Cronin, C.-H. Tung and Y. F. Wang, *J. Am. Chem. Soc*., 2016, **138**, 11097−11100.
7. Q. Sun, C. Y. Liu, G. Y. Zhang, J. Zhang, C.-H. Tung and Y. F. Wang, *Chem. Eur. J*., 2018, **24**, 14701–14706.
8. S. Øien-Ødegaard, C. Bazioti, E. A. Redekop, Ø. Prytz, K. P. Lillerud and U. Olsbye, *Angew. Chem. Int. Ed*., 2020, **59**, 21397–21402.
9. Y. Mouri, Y. Sakai, Y. Kobayashi, S. Yoshida and K. Nomiya, *Materials*, 2010, **3**, 503−518
10. Y. H. Ren, S. X. Liu, R. G. Cao, X. Y. Zhao, J. F. Cao and C. Y. Gao, *Inorg. Chem. Commun*., 2008, **11**, 1320−1322.
11. H. T. Chen, L. M. Fan and X. T. Zhang, *ACS Appl. Mater. Interfaces.,* 2020, **12**, 54884–54892.
12. S. R. Liu, H. T. Chen, L. M. Fan and X. T. Zhang, *Inorg. Chem*., 2023, **62**, 3562–3572.
13. W. M. Chen, N. Xu, L. Qin, Y. F. Deng, G. L. Zhuang, Z. Zhang, T. Z. Xie, P. S. Wang and Z. P. Zheng, *Angew. Chem. Int. Ed.*, 2025, **64**, e202420770.
14. X. Y. Zhang, Y. R. Li, L. H. Hong, P. X. Wu, Y. C. Cong, Y. H. Mi, Y. Q. Sun, S. T. Zheng and X. X. Li, *J. Solid State Chem.,* 2025, 347, 125304.
15. T. Y. Dang, H. R. Tian, Y. Lu, R. H. Li and S. X. Liu, *Appl. Surf. Sci.,* 2024, **654**, 159459.
16. A. Yoshida, S. Hikichi and N. Mizuno, *J. Organomet. Chem.,* 2007, **692**, 455–459.
17. S. Zhao, Y. Chen and Y. F. Song, *Appl. Catal. A Gen.,* 2014, **475**, 140–146.
18. H. L. Li, S. H. Zhao, Y. M. Chen, C. Lian and X. H. Cao, *Inorg. Chem. Commun*., 2024, **170**, 113441.
19. C. R. Wang, H. L. Li, Z. W. Wang, Y. W, J. N. Zhao, J. Chen, M. Z. Jia and G. Y. Yang, *Inorg. Chem.*, 2026, **65**, 5148–5155.